

1 A comparison of the effect of molluscum contagiosum virus MC159 and MC160 proteins on
2 vaccinia virus virulence in intranasal and intradermal infection routes

3

4 Sunetra Biswas^a, Geoffrey L. Smith^b, Edward J. Roy^c, Brian Ward^d, Joanna L. Shisler^{a*}

5

6 sbiswas4@illinois.edu, jshisler@illinois.edu, Department of Microbiology, University of Illinois,

7 Urbana IL 61801 USA

8 gls37@cam.ac.uk, Department of Pathology, Cambridge University, Tennis Court Road,

9 Cambridge, UK

10 eroy@illinois.edu, Department of Molecular and Integrative Physiology, University of Illinois,

11 Urbana IL 61801 USA

12 Brian_Ward@URMC.Rochster.edu, Department of Microbiology and Immunology, University of

13 Rochester, Rochester, NY USA

14

15 *corresponding author

16

17

18 running title: The MCV MC159 protein decreases the virulence of vaccinia virus

19

20

21

22

23

24

25

26

27 **Abstract**

28 Molluscum contagiosum virus (MCV) causes persistent, benign skin neoplasm in children and
29 adults. MCV is refractive to growth in standard tissue culture and there is no relevant animal
30 model of infection. Here we investigated if another poxvirus (vaccinia virus; VACV) could be
31 used to examine MCV immunoevasion protein properties *in vivo*. The MCV *MC159L* or *MC160L*
32 gene, which encode NF- κ B antagonists, were inserted into an attenuated VACV lacking an NF-
33 κ B antagonist ($v\Delta A49$), creating *vMC159* and *vMC160*. *vMC160* slightly increased $v\Delta A49$
34 virulence in the intranasal and intradermal routes of inoculation. *vMC159* infection was less
35 virulent than $v\Delta A49$ in both inoculation routes. *vMC159*-infected ear pinnae did not form lesions,
36 but virus replication still occurred. Thus, the lack of lesions was not due to abortive virus
37 replication. This system provides a new approach to examine MCV immunoevasion proteins
38 within the context of a complete and complex immune system.

39

40

41

42

43

44

45

46

47

48

49

50

51

52 Molluscum contagiosum virus (MCV) is dermatotropic poxvirus, and is the etiological
53 agent of molluscum contagiosum (MC) [1]. MCV infections are common and worldwide [2, 3].
54 MCV infects keratinocytes and infections can persist for months to years [4]. MC neoplasms are
55 small and have little inflammation associated with them [1]. Lesions that spontaneously regress
56 have increased numbers of apoptosing cells, cytotoxic T cells, natural killer cells, and type I IFN-
57 expressing plasmacytoid dendritic cells [5]. Thus, it is presumed that one key to MCV
58 persistence lies in MCV modulating the host response.

59 Very little is known about MCV immune evasion strategies as compared to other viruses.
60 This is because MCV is refractive to growth in standard tissue culture. The sequencing of the
61 MCV genome revealed that MCV encodes at least 40 known or predicted immune evasion
62 molecules [6, 7]. Several of these proteins were characterized by studying them independent of
63 MCV infection [4, 8-11]. However, it remains unknown how these MCV immune evasion
64 molecules play a role in viral pathogenesis.

65 To overcome this technical barrier, we chose to deliver MCV immune evasion proteins
66 (MC159 and MC160) to mice during a related poxvirus (VACV) infection. MC159 and MC160
67 were examined because each protein inhibits NF- κ B activation, yet each uses different
68 mechanisms to antagonize the NF- κ B activation pathway [12-15]. We chose VACV because it is
69 the best-studied poxvirus [16], and there are several excellent animal models of VACV infection
70 that afford studying the impact of viral immune evasion molecules on viral pathogenesis [17-20].
71 Additionally, we published that MC159 and MC160 inhibit NF- κ B and IRF3 activation in murine
72 cell lines [21]. Further, Randall et al show that MC159 interacts with murine NEMO [15]. We
73 also have unpublished data showing that MC160 induces murine IKK1 degradation, similar to
74 MC160's effect on human IKK1 [13, 14]. Thus, even though MCV is a human pathogen, it is
75 likely that MC159 and MC160 interact with some of the known equivalent murine binding
76 partners involved in immune surveillance.

77 VACV strain vΔA49 was used as the parental virus, Fig. 1(a). vΔA49 lacks A49, which is
78 an NF-κB antagonist [22]. We chose this virus because vΔA49 is moderately decreased in
79 virulence [22], and because MC159 and MC160 are reported to inhibit NF-κB activation [12, 14,
80 15]. Furthermore, MC159 and MC160 each act upstream of A49 [12, 14, 15, 22]. Thus, insertion
81 of MC159 or MC160 into vΔA49 might restore vΔA49 virulence.

82 The *MC159L* and *MC160L* genes were stably inserted into vΔA49, a virus construct that
83 deleted nucleotides 113-473 of the *A49R* gene [22], Fig. 1(a). The expression of *MC159L* and
84 *MC160L* was controlled by the VACV p7.5 promoter to ensure MCV gene expression
85 throughout VACV infection. Of course, the expression profile for these MCV genes in VACV
86 may differ from that of its profile during a natural MCV infection. The creation of vMC159 was
87 described previously [12]. The strategy for constructing vMC160 was similar.

88 To create vMC160, an *MC160L* gene under the control of the VACV p7.5 promoter was
89 inserted into the pΔA49MCS plasmid [12]. pΔA49MCS contains a mutated *A49R* gene lacking nt
90 113-473 that is flanked by a portion of the *A48R* and *A50R* genes [12]. The *A48* flank begins at
91 *A48R* nt 457 and continues through to *A49R* nt 112 for a 338-bp product [12]. It also possesses
92 multiple cloning sites for insertion of the *MC160L* gene [12]. To create MC160/pΔA49MCS, the
93 *MC160L* gene was PCR amplified from MC160/pCI [13] using forward primer 5'-
94 **GGATCTATAATCATGGCGCACGAGCCA** -3' and reverse primer 5'-
95 **CTAGACTAGTCTAGTAGGAAGCTTTCGTT**-3'
96 to yield a 1212-bp PCR product. The MC160 nucleotides are underlined. The reverse primer
97 for MC160 engineered in the *Spe* I restriction enzyme digestion site (italicized). The p7.5
98 promoter was PCR amplified from pUC13/gpt/EGFP [22], yielding a 121-bp product. The
99 forward primer was 5'-TTTTATCGATTAAATAATAAATACAATAATTAATTTCTCGT-3' and the
100 reverse primer was 5'- **CTCGTGCGCCATGATTATAGATCCGTC**ACTG-3'and this yielded a
101 121-bp PCR product. The forward primer introduced a *Clal* restriction enzyme site (italicized).

102 Next, 50-100 ng of the gel-purified PCR products were joined by SOE, and PCR amplified using
103 the A48R forward and A50R reverse primers described in Biswas et al [12]. The resultant PCR
104 product (1433 bp) was digested with *ClaI* and *SpeI* and inserted into pΔA49MCS that had been
105 digested with *ClaI* and *SpeI* and treated with SAP. This plasmid was named
106 MC160/pΔA49MCS.

107 To create vMC160, CV-1 cells were infected with vΔA49 and transfected with pMC160
108 and transient dominant selection was used, as described previously [23]. Recombinant viruses
109 were collected 24 h later selected in the presence of mycophenolic acid, xanthine and
110 hypoxanthine [23]. This process was repeated three times to isolate recombinant viruses away
111 from parental viruses. Intermediate EcoGPT⁺ viruses were resolved into vMC160 by plaquing on
112 BSC-1 cells in the absence of drugs.

113 As shown in Fig. 1(b), the genotype of vMC160 was confirmed by using PCR analysis.
114 Note that the 362-bp amplicon from vΔA49-infected cells increased in size to 1,692 bp,
115 reflecting insertion of the 883-bp and 1,333-bp *MC160L* insert. Similarly, there was an 883-bp
116 product when PCR amplifying the region flanking *MC159L*, as expected. Finally, the 55-kDa
117 MC160 protein expression was detected in infected cells as early as 2 h (post-infection) p.i. and
118 remained detectable at 24 h p.i. using polyclonal antiserum specific MC160 [24], Fig. 1(c). As
119 previously reported, the 31-kDa MC159 protein was also detected using anti-MC159 antiserum.
120 The VACV E3 protein, an early protein, was detected throughout infection, as predicted [25].
121 Actin levels were similar in each lane, showing even protein loading.

122 Intranasal (IN) inoculation allows examination of VACV virulence; VACV initially infects
123 the lungs and then spreads to the brain and other distal organs [17, 26]. BALB/c mice were
124 inoculated IN with 5×10^3 p.f.u. of a virus as described [27]. Mice were examined daily and we
125 used a 5-point scoring system that determines the extent of illness [28, 29]. This was performed
126 as a blinded study to minimize potential bias. We only analyzed the planned comparisons of

127 vΔA49 to either vMC159, vMC160 or vΔA49rev, and set *P* values of <0.05 (indicated by one
128 asterisk), *P* <0.01 (as indicated by two asterisks) and *P* < 0.0001 (as indicated by 4 asterisks)
129 as criteria for statistical significance for these and the remaining assays involving mice.

130 PBS-inoculated mice showed no signs of illness at any time point. vΔA49rev, which is
131 equivalent to wild type VACV strain WR, triggered clinical signs of illness similar to results
132 reported previously [22] (Fig. 2A). vΔA49 infection delayed illness onset, and clinical scores
133 were consistently lower than vΔA49rev-infected mice as noted previously [22]. These
134 differences were statistically significant on days 7-13 p.i. (Fig. 2A). vMC159 infection appeared
135 to cause a milder disease; the clinical scores from vMC159-infected mice were lower than
136 vΔA49-infected mice from days 8 -12 p.i., and these differences were statistically significant on
137 days 8, 9, and 11-13 post-infection, Fig. 2(a). In comparison to vΔA49 infection, mice infected
138 with vMC160 had increased signs of illness, Fig. 2(a). These differences were statistically
139 significant at days 7 and 8 post-infection, Fig. 2(a). These data suggest that the *MC159L* gene
140 reduced the virulence of vΔA49 while *MC160L* partially substituted for *A49L*.

141 Weight loss is an additional measure of virus virulence for IN inoculations [30]. The
142 same mice as in Fig. 2(a) were also weighed daily, and data were expressed as the percentage
143 of the mean of each individual animal's weight loss from day 0 +/- SEM [27]. Results are shown
144 in Fig. 2(b). We only analyzed the planned comparisons of vΔA49 to either vMC159, vMC160 or
145 vΔA49rev. vΔA49rev infection caused weight loss similar to that reported previously [22].
146 vΔA49-infected mice lost less weight than vΔA49rev-infected mice as expected [22], and these
147 differences were statistically significant on days 8-12 p.i., Fig. 2(b). vMC159 caused less weight
148 loss than vΔA49 at days 8-15 p.i. although these differences in weight were not statistically
149 significant. vMC160-infected mice also weighed slightly more than vΔA49-infected mice at days
150 8-12 p.i., but these differences were not statistically significant. These data suggested that
151 MC159 decreased virus virulence to a greater extent than vMC160 in the IN infection model.

152 The intradermal (ID) inoculation of a mouse ear pinna provides an alternative model to
153 examine VACV virulence [19, 31]. In this case, lesion formation and lesion size is used to
154 quantify virulence [18]. One could argue that ID inoculations most closely represent the location
155 of natural, dermatotropic MCV infections. There also are some parallels in the immune
156 responses to ID VACV infections and MCV infections. For example, type I IFN appears to be
157 important in controlling lesion size in VACV-infected ears [32] and lesion resolution during MCV
158 infections [5].

159 For ID inoculations, C57BL/6 mice were inoculated ID in the left ear dorsal pinna with
160 10^4 PFU of each virus as described in [27]. The infected ears were examined daily for the next
161 18 days for the presence of lesions, and results are shown in Fig. 3(a). We only analyzed the
162 planned comparisons of $v\Delta A49$ to either $vMC159$, $vMC160$ or $v\Delta A49rev$. For all virus infections,
163 no lesions were visually detected for the first six days p.i., a routine observation [27]. Gross
164 lesions were observed in $v\Delta A49rev$ -infected mice starting on day 7 p.i., and lesion size
165 increased until day 12, and then resolved from days 13-18. $v\Delta A49$ -induced lesion sizes were
166 slightly smaller than $v\Delta A49rev$ at all times examined, and were statistically significant only on
167 days 10 and 11 p.i. $vMC160$ -associated lesions were similar in size to lesions produced by
168 $v\Delta A49rev$ and slightly larger than $v\Delta A49$ -induced lesions. When comparing lesions from
169 $vMC160$ - versus $v\Delta A49$ -infected mice, $vMC160$ lesions were significantly larger on days 7,8 and
170 10 p.i., indicating that $MC160$ may increase virulence partially. Surprisingly, $vMC159$ inoculation
171 did not produce a lesion at any point in time, Fig 3(a) and (b).

172 The most striking results observed were those for the ID model of infection, and that
173 there was a complete lack of lesion formation during $vMC159$ infection. Only 2 other VACV
174 strains have been reported to not cause lesion formation in skin: $v\Delta A36R$ and NYVAC [18, 33].
175 $v\Delta A36R$ and NYVAC cannot spread from cell-to-cell efficiently *in vitro* [18, 33, 34]. It is thought

176 that $\Delta A36R$ or NYVAC do not cause lesions because they spread less efficiently to neighboring
177 cells *in vivo*, resulting in an abortive infection process.

178 One question was why vMC159 would cause no lesions. vMC159 and vMC160 each
179 replicated to the same levels as v $\Delta A49$ using either one-step or multi-step growth curve assays
180 in mouse embryo fibroblasts (MEFs) (data not shown). Also, vMC159- and vMC160-formed
181 plaques were similar to v $\Delta A49$ and vA49 in MEF and BSC40 cellular monolayers (data not
182 shown). Thus, it was unlikely that vMC159 spreads less efficiently for reason suspected for
183 v $\Delta A36R$ and NYVAC. Another possibility was that MC159 and MC160 may not interact with the
184 murine homologs of their binding partners. This is also unlikely because MC159 interacts with
185 murine NEMO [15] and MC160 interacts with murine IKK1 (data not shown). Next, viral titers
186 were quantified at 3, 5 and 11 days p.i. [27]. Maximum VACV titers are detected at day 5 p.i.
187 [19], and we chose these time points to detect virus replication prior to and after maximal
188 replication. vMC160 titers were not examined because vMC160-induced ear lesions were
189 similar to those for v $\Delta A49$ and v $\Delta A49$ rev.

190 Data are shown in Figure 3 as both p.f.u. per ear Fig. 3(c) and PFU per gram of tissue
191 Fig. 3(d). The starting inoculum was 10^4 p.f.u. in each ear pinna [27]. Data showed that all
192 viruses replicated because virus titers were higher than the initial inoculum (10^4 p.f.u.) on days 3
193 and 5 p.i. vMC159 titers were lower than the wild-type (vA49rev) or parental (v $\Delta A49$) viruses at
194 all times tested. v $\Delta A49$ and v $\Delta A49$ rev titers increased to approximately 1.3×10^6 by day 3 p.i.
195 (Fig. 3C). In contrast, vMC159 titers were 1.2×10^5 p.f.u. at day 3 p.i. All viruses continued to
196 replicate during the next 48 h because titers increased between 3 and 5 days p.i. By day 11 p.i.,
197 virus replication had waned, as indicated by the decrease in virus titers. Note that the decrease
198 in virus titers from day 5 to day 11 p.i. implies that there is indeed immune mediated clearance
199 of virus, but this occurred without accompanying inflammation.

200 One could argue that no lesions arise because vMC159 titers are lower than vΔA49 in
201 ear pinnae. Indeed, it is unclear what the threshold of virus titer is needed for lesion formation.
202 Tscharke *et al.* showed that inoculation with as little as 10^2 p.f.u. of VACV induces ear lesions
203 formation [18]. vMC159 titers greatly exceed that amount at days 3 and 5 p.i. This suggests that
204 vMC159 decouples replication from lesion formation. Interestingly, both ΔA36R and NYVAC
205 elicit protective immune responses (e.g., antibody production) [18, 35]. Thus, it is tempting to
206 ask if vMC159 also retains its immunogenicity and, if so, if vMC159 would be useful for the
207 vaccine field.

208 It is not yet clear how MC159 suppresses lesion formation, and this is a direction for
209 future studies. It is appreciated that VACV lesions are due, in part, to immunopathology
210 because smaller lesions are associated with decreases in expression of multiple cytokines and
211 chemokines [27, 36]. Thus, MC159 may either directly or indirectly prevent expression of these
212 host cell proteins to halt pro-inflammatory processes. In this case, the MC159 ability to inhibit
213 NF-κB and IRF3 activation may be relevant. MC159 inhibits apoptosis while MC160 does not
214 [24, 37]. Another speculation, then, is that this anti-apoptotic property of MC159 affords virus
215 attenuation, perhaps by allowing virus-infected cells to survive for longer time periods.
216 Interestingly, a mutant VACV lacking an apoptosis antagonist (ΔB13R) has an increased lesion
217 size as compared to wild-type VACV [18], showing an instance where inhibition of apoptosis
218 diminishes lesion formation.

219 This is the first report that examines MCV immune antagonists in the context of an animal
220 infection. MC159 and MC160 are members of the FLIP family of proteins [4]. They each
221 possess tandem death effector domains (DEDs) that share 43% similarity. MC159 and MC160
222 also share some biological features, including inhibition of NF-κB and IRF3 [4]. Despite their
223 similarity, MC159 and MC160 likely have distinct roles during MCV infection *in vivo*, as indicated
224 by data here. VACV itself expresses at least 10 different NF-κB inhibitory proteins [20],

225 indicating that control of this pathway is critical for survival of VACV *in vivo*. Perhaps MCV also
226 expresses MC159 and MC160, along with the two other known MCV NF- κ B antagonists
227 (MC005, MC132), for similar reasons when confronting a complex, multi-faceted anti-viral
228 immune response [10, 11].

229 To date, there is no cell culture system or laboratory animal model to study MCV
230 replication and pathogenesis. Researchers have used creative approaches to extrapolate the
231 biological importance of MC159 as an immune evasion molecule. This includes the
232 development of transgenic mouse strains that express MC159 [38, 39] or using murine
233 cytomegalovirus to express MC159 [40]. Our system uses VACV during ID mouse infections,
234 and is perhaps the model closest to mimicking MCV infection at this current time. One could
235 argue that the addition of MC159 to v Δ A49 resulted in a disease that mimics MC because, like
236 MC, there is little inflammation.

237 The current study demonstrates the biological effects of two well-characterized MCV
238 immune evasion proteins in a newly-created system. MCV encodes at least 40 other known or
239 predicted immune evasion molecules [6, 7]. Thus, studies of MCV immune evasion molecules
240 provide a rich opportunity to identify novel aspects of virus-host interactions during persistent
241 infections. The surrogate system described here now affords these types of studies to better
242 understand MCV pathogenesis and persistent virus infections.

243

244

245

246

247

248

249

250 **Figure Legends**

251 **Figure 1. Characterization of vaccinia viruses expressing either MC159 or MC160.** (A) A
252 schematic of the viruses used in this study, focusing on the portion of the VACV WR genome
253 containing the *A49R* gene and portions of the *A48R* and *A50R* genes flanking *A49R*. v Δ A49 is a
254 VACV strain in which *A49R* nucleotides 113-473 are deleted. Either the MCV *MC159L* or the
255 *MC160L* genes, each under the control of the VACV p7.5 promoter, were inserted into v Δ A49 to
256 create vMC159 or vMC160, respectively. U5NU is the early gene transcription termination
257 signal. (B) BSC40 monolayers were either mock-infected or infected with the indicated viruses
258 (MOI = 10). At 24 h p.i., cells were collected, and DNA was isolated. DNA was PCR amplified
259 using a forward primer specific for *A48R* and reverse primer specific for *A50R* [22]. A portion of
260 each PCR reaction was analyzed by gel electrophoresis. Bands were detected by ethidium
261 bromide staining of the gel. (C) BSC40 monolayers were either mock-infected or with v Δ A49,
262 vMC159 or vMC160 (MOI = 10). Cells were lysed at the indicated times and 15 μ g of clarified
263 cellular lysates were subjected to immunoblotting for the presence of MCV (MC159, MC160) or
264 VACV (E3) proteins or cellular β -actin.

265
266 **Figure 2. The effect of MCV genes on virus virulence using the intranasal route of**
267 **infection.** Female BALB/c mice (n = 5 per group) were inoculated IN with 5 X 10³ p.f.u. v Δ A49,
268 v Δ A49rev, vMC159, or vMC160 or PBS. (A) Clinical signs of illness were monitored daily for 15
269 days and scored from 0-5. Clinical scores were expressed as the mean for each group. One-
270 way ANOVA was performed followed by Tukey's multiple comparison test to determine
271 statistical significance. Asterisks indicate the days on which clinical signs of illness induced were
272 significantly different between the indicated groups. (**P* < 0.05, ***P* < 0.01 or *****P* < 0.0001).
273 (B) Mice were weighed daily, and data were expressed as the percentage of weight change
274 from day 0. To determine statistically significant differences between weight change during virus

275 infection, two-way analysis of variance (ANOVA), followed by Tukey's multiple comparison test,
276 was performed. Asterisks indicate the days on which weight change induced by vΔA49 were
277 significantly different from those induced by vΔA49rev (**P* < 0.05).

278

279 **Figure 3. The effect of MCV genes on virus virulence using the intradermal route of**
280 **inoculation.** C57BL/6 mice (n = 5 per group) were infected ID with 10⁴ p.f.u. vΔA49, vΔA49rev,
281 vMC159, or vMC160 in the left ear pinna. Lesion size was expressed as the mean for the group
282 +/- SEM. (A) Sizes of resulting lesions were measured daily for 18 days. The lesion size was
283 measured by using a 0.01-mm digital caliper. The data are expressed as the means of lesion
284 sizes ±SEM. Statistical significance was determined by two-way ANOVA, followed by Tukey's
285 multiple comparison test. The asterisks indicate the days on which the lesion size caused was
286 statistically significantly between indicated groups (**P* < 0.05 or *****P* < 0.0001). (B)
287 Representative images of inoculated ear pinnae at 10 days p.i. vΔA49-infected mice (left panel)
288 or vMC159-infected mice (right panel). (C and D) At the indicated days p.i., ears were collected,
289 homogenized, and lysed, and viral titers of the lysates were determined by plaque assay. Each
290 symbol represents the virus titer from an individual animal, and the mean titer is indicated by a
291 line. Data are expressed as the mean titer of virus (p.f.u.) per gram of tissue (D) and as the total
292 p.f.u. per ear (C). Statistical significance was determined by Kruskal-Wallis test. The asterisk
293 indicate data points at which titers of viruses were statistically significantly different from the
294 other (**P* < 0.05).

295

296

297

298

299

300 **Funding information**

301 This work was supported by grants from the University of Illinois Campus Research Board and
302 the National Institutes of Health (AI117105). GLS is a Wellcome Trust Principal Research
303 Fellow.

304

305 **Acknowledgements**

306 The authors thank Dr. Ariana Bravo Cruz, Lauren Gates and Melissa Ryerson for advice and
307 review.

308

309 **Ethical Statement**

310 The work described was undertaken with ethical approval from the University of Illinois IACUC.

311

312 **Conflicts of interest.**

313 The authors declare that there are no conflicts of interest that they are aware of.

314

315

316

317

318

319

320

321

322

323

324

325

326 **References**

327

- 328 1. **Damon IK.** Poxviruses. In: Fields BN, Knipe DM, Howley PM (editors). *Fields virology*.
329 Philadelphia: Wolters Kluwer Health/Lippincott Williams & Wilkins; 2013. pp. 2160-2184.
- 330 2. **Hay RJ, Johns NE, Williams HC, Bolliger IW, Dellavalle RP et al.** The global burden
331 of skin disease in 2010: an analysis of the prevalence and impact of skin conditions. *The*
332 *Journal of investigative dermatology* 2014;134(6):1527-1534.
- 333 3. **Gottlieb SL, Myskowski PL.** Molluscum contagiosum. *Int J Dermatol* 1994;33(7):453-
334 461.
- 335 4. **Shisler JL.** Immune evasion strategies of molluscum contagiosum virus. *Adv Virus Res*
336 2015;92:201-252.
- 337 5. **Vermi W, Fisogni S, Salogni L, Scharer L, Kutzner H et al.** Spontaneous regression
338 of highly immunogenic Molluscum contagiosum virus (MCV)-induced skin lesions is associated
339 with plasmacytoid dendritic cells and IFN-DC infiltration. *The Journal of investigative*
340 *dermatology* 2011;131(2):426-434.
- 341 6. **Senkevich TG, Bugert JJ, Sisler JR, Koonin EV, Darai G et al.** Genome sequence of
342 a human tumorigenic poxvirus: prediction of specific host response-evasion genes. *Science*
343 1996;273(5276):813-816.
- 344 7. **Senkevich TG, Koonin EV, Bugert JJ, Darai G, Moss B.** The genome of molluscum
345 contagiosum virus: analysis and comparison with other poxviruses. *Virology* 1997;233(1):19-42.
- 346 8. **Chen X, Anstey AV, Bugert JJ.** Molluscum contagiosum virus infection. *The Lancet*
347 *infectious diseases*, Research Support, Non-U.S. Gov't
348 Review 2013;13(10):877-888.
- 349 9. **Coutu J, Ryerson MR, Bugert JJ, Nichols DB.** The Molluscum Contagiosum Virus
350 protein MC163 localizes to the mitochondria and dampens mitochondrial mediated apoptotic
351 responses. *Virology* 2017;in press.

- 352 10. **Brady G, Haas DA, Farrell PJ, Pichlmair A, Bowie AG.** Molluscum Contagiosum Virus
353 Protein MC005 Inhibits NF-kappaB Activation by Targeting NEMO-Regulated I kappa B Kinase
354 Activation. *Journal of virology* 2017;91(15).
- 355 11. **Brady G, Haas DA, Farrell PJ, Pichlmair A, Bowie AG.** Poxvirus Protein MC132 from
356 Molluscum Contagiosum Virus Inhibits NF-B Activation by Targeting p65 for Degradation.
357 *Journal of virology* 2015;89(16):8406-8415.
- 358 12. **Biswas S, Shisler JL.** Molluscum Contagiosum Virus MC159 Abrogates cIAP1-NEMO
359 Interactions and Inhibits NEMO Polyubiquitination. *Journal of virology* 2017;91(15).
- 360 13. **Nichols DB, Shisler JL.** The MC160 protein expressed by the dermatotropic poxvirus
361 molluscum contagiosum virus prevents tumor necrosis factor alpha-induced NF-kappaB
362 activation via inhibition of I kappa kinase complex formation. *Journal of virology* 2006;80(2):578-
363 586.
- 364 14. **Nichols DB, Shisler JL.** Poxvirus MC160 protein utilizes multiple mechanisms to inhibit
365 NF-kappaB activation mediated via components of the tumor necrosis factor receptor 1 signal
366 transduction pathway. *Journal of virology* 2009;83(7):3162-3174.
- 367 15. **Randall CM, Jokela JA, Shisler JL.** The MC159 protein from the molluscum
368 contagiosum poxvirus inhibits NF-kappaB activation by interacting with the I kappa B kinase
369 complex. *J Immunol* 2012;188(5):2371-2379.
- 370 16. **Moss B.** *Poxviridae* 6th ed: Lippincott Williams & Wilkins 2013.
- 371 17. **Reading PC, Smith GL.** A kinetic analysis of immune mediators in the lungs of mice
372 infected with vaccinia virus and comparison with intradermal infection. *The Journal of general*
373 *virology* 2003;84(Pt 8):1973-1983.
- 374 18. **Tscharke DC, Reading PC, Smith GL.** Dermal infection with vaccinia virus reveals
375 roles for virus proteins not seen using other inoculation routes. *The Journal of general virology*
376 2002;83(Pt 8):1977-1986.

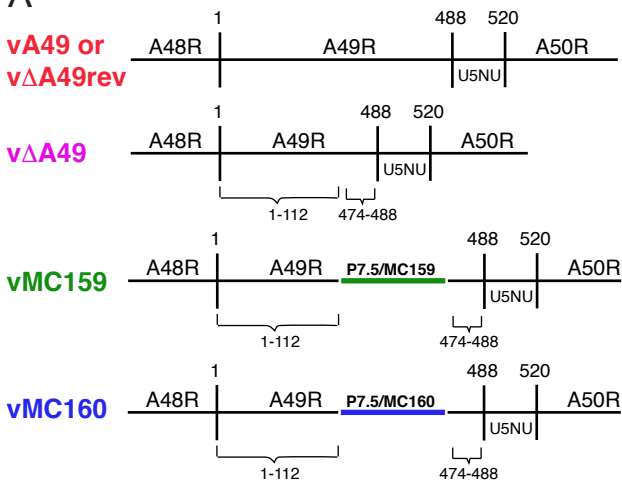
- 377 19. **Tscharke DC, Smith GL.** A model for vaccinia virus pathogenesis and immunity based
378 on intradermal injection of mouse ear pinnae. *The Journal of general virology* 1999;80 (Pt
379 10):2751-2755.
- 380 20. **Smith GL, Benfield CT, Maluquer de Motes C, Mazzon M, Ember SW et al.** Vaccinia
381 virus immune evasion: mechanisms, virulence and immunogenicity. *The Journal of general*
382 *virology* 2013;94(Pt 11):2367-2392.
- 383 21. **Randall CM, Biswas S, Selen CV, Shisler JL.** Inhibition of interferon gene activation by
384 death-effector domain-containing proteins from the molluscum contagiosum virus. *Proceedings*
385 *of the National Academy of Sciences of the United States of America* 2014;111(2):E265-272.
- 386 22. **Mansur DS, Maluquer de Motes C, Unterholzner L, Sumner RP, Ferguson BJ et al.**
387 Poxvirus targeting of E3 ligase beta-TrCP by molecular mimicry: a mechanism to inhibit NF-
388 kappaB activation and promote immune evasion and virulence. *PLoS pathogens*
389 2013;9(2):e1003183.
- 390 23. **Falkner FG, Moss B.** Transient dominant selection of recombinant vaccinia viruses.
391 *Journal of virology* 1990;64(6):3108-3111.
- 392 24. **Shisler JL, Moss B.** Molluscum contagiosum virus inhibitors of apoptosis: The MC159
393 v-FLIP protein blocks Fas-induced activation of procaspases and degradation of the related
394 MC160 protein. *Virology* 2001;282(1):14-25.
- 395 25. **Weaver JR, Shamim M, Alexander E, Davies DH, Felgner PL et al.** The identification
396 and characterization of a monoclonal antibody to the vaccinia virus E3 protein. *Virus research*
397 2007;130(1-2):269-274.
- 398 26. **Alcami A, Smith GL.** A mechanism for the inhibition of fever by a virus. *Proceedings of*
399 *the National Academy of Sciences of the United States of America* 1996;93(20):11029-11034.
- 400 27. **Bravo Cruz AG, Han A, Roy EJ, Guzman AB, Miller RJ et al.** Deletion of the K1L
401 Gene Results in a Vaccinia Virus That Is Less Pathogenic Due to Muted Innate Immune
402 Responses, yet Still Elicits Protective Immunity. *Journal of virology* 2017;91(15).

- 403 28. **Berhanu A, King DS, Mosier S, Jordan R, Jones KF et al.** ST-246 inhibits in vivo
404 poxvirus dissemination, virus shedding, and systemic disease manifestation. *Antimicrobial*
405 *agents and chemotherapy* 2009;53(12):4999-5009.
- 406 29. **Alcami A, Smith GL.** A soluble receptor for interleukin-1 beta encoded by vaccinia
407 virus: a novel mechanism of virus modulation of the host response to infection. *Cell*
408 1992;71(1):153-167.
- 409 30. **Williamson JD, Reith RW, Jeffrey LJ, Arrand JR, Mackett M.** Biological
410 characterization of recombinant vaccinia viruses in mice infected by the respiratory route. *The*
411 *Journal of general virology* 1990;71 (Pt 11):2761-2767.
- 412 31. **Lin LC, Smith SA, Tschärke DC.** An intradermal model for vaccinia virus pathogenesis
413 in mice. *Methods Mol Biol* 2012;890:147-159.
- 414 32. **Fischer MA, Davies ML, Reider IE, Heipertz EL, Epler MR et al.** CD11b(+), Ly6G(+)
415 cells produce type I interferon and exhibit tissue protective properties following peripheral virus
416 infection. *PLoS pathogens* 2011;7(11):e1002374.
- 417 33. **Tartaglia J, Perkus ME, Taylor J, Norton EK, Audonnet JC et al.** NYVAC: a highly
418 attenuated strain of vaccinia virus. *Virology* 1992;188(1):217-232.
- 419 34. **Parkinson JE, Smith GL.** Vaccinia virus gene A36R encodes a M(r) 43-50 K protein on
420 the surface of extracellular enveloped virus. *Virology* 1994;204(1):376-390.
- 421 35. **Tartaglia J, Cox WI, Pincus S, Paoletti E.** Safety and immunogenicity of recombinants
422 based on the genetically-engineered vaccinia strain, NYVAC. *Dev Biol Stand* 1994;82:125-129.
- 423 36. **Stanford MM, McFadden G, Karupiah G, Chaudhri G.** Immunopathogenesis of
424 poxvirus infections: forecasting the impending storm. *Immunol Cell Biol* 2007;85(2):93-102.
- 425 37. **Shisler JL, Senkevich TG, Berry MJ, Moss B.** Ultraviolet-induced cell death blocked
426 by a selenoprotein from a human dermatotropic poxvirus. *Science* 1998;279(5347):102-105.

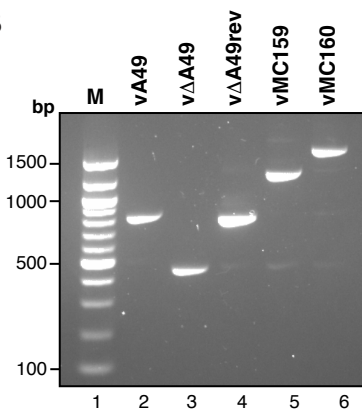
- 427 38. **Woelfel M, Bixby J, Brehm MA, Chan FK.** Transgenic expression of the viral FLIP
428 MC159 causes lpr/gld-like lymphoproliferation and autoimmunity. *J Immunol* 2006;177(6):3814-
429 3820.
- 430 39. **Wu Z, Roberts M, Porter M, Walker F, Wherry EJ et al.** Viral FLIP impairs survival of
431 activated T cells and generation of CD8+ T cell memory. *J Immunol* 2004;172(10):6313-6323.
- 432 40. **Huttmann J, Krause E, Schommartz T, Brune W.** Functional Comparison of
433 Molluscum Contagiosum Virus vFLIP MC159 with Murine Cytomegalovirus M36/vICA and
434 M45/vIRA Proteins. *Journal of virology* 2015;90(6):2895-2905.
- 435

Figure 1.

A



B



C

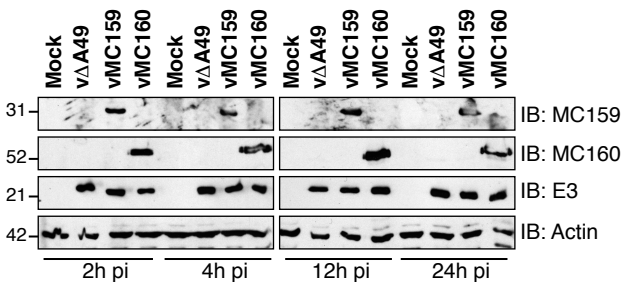
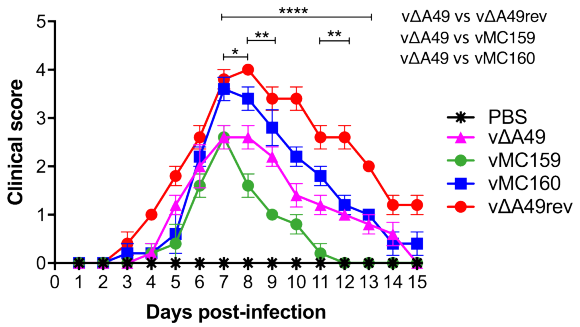


Figure 2.

A



B

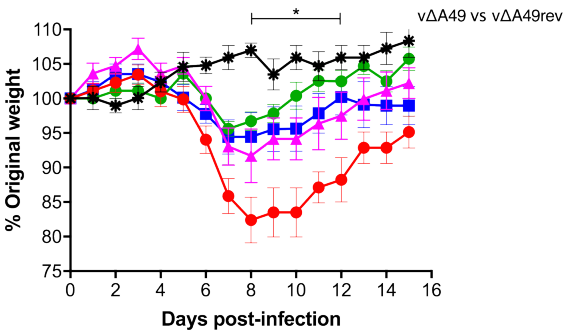
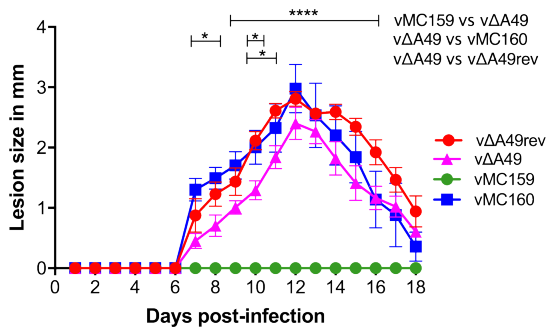
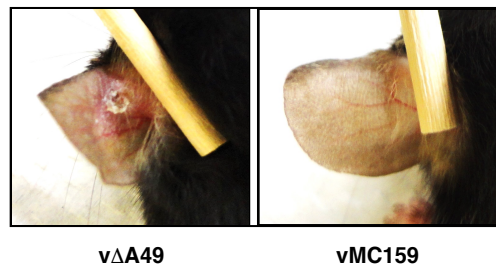


Figure 3.

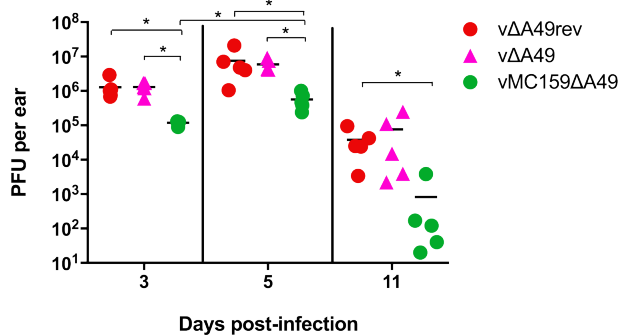
A



B



C



D

